

Mitochondrial H₂O₂ emission and cellular redox state link excess fat intake to insulin resistance in both rodents and humans

Ethan J. Anderson, ... , David H. Wasserman, P. Darrell Neuffer

J Clin Invest. 2009;119(3):573-581. <https://doi.org/10.1172/JCI37048>.

Research Article

Metabolism

High dietary fat intake leads to insulin resistance in skeletal muscle, and this represents a major risk factor for type 2 diabetes and cardiovascular disease. Mitochondrial dysfunction and oxidative stress have been implicated in the disease process, but the underlying mechanisms are still unknown. Here we show that in skeletal muscle of both rodents and humans, a diet high in fat increases the H₂O₂-emitting potential of mitochondria, shifts the cellular redox environment to a more oxidized state, and decreases the redox-buffering capacity in the absence of any change in mitochondrial respiratory function. Furthermore, we show that attenuating mitochondrial H₂O₂ emission, either by treating rats with a mitochondrial-targeted antioxidant or by genetically engineering the overexpression of catalase in mitochondria of muscle in mice, completely preserves insulin sensitivity despite a high-fat diet. These findings place the etiology of insulin resistance in the context of mitochondrial bioenergetics by demonstrating that mitochondrial H₂O₂ emission serves as both a gauge of energy balance and a regulator of cellular redox environment, linking intracellular metabolic balance to the control of insulin sensitivity.

Find the latest version:

<https://jci.me/37048/pdf>



Mitochondrial H₂O₂ emission and cellular redox state link excess fat intake to insulin resistance in both rodents and humans

Ethan J. Anderson,^{1,2,3} Mary E. Lustig,⁴ Kristen E. Boyle,^{1,2} Tracey L. Woodlief,^{1,2} Daniel A. Kane,^{1,2} Chien-Te Lin,^{1,2} Jesse W. Price III,⁵ Li Kang,⁴ Peter S. Rabinovitch,⁶ Hazel H. Szeto,⁷ Joseph A. Houmard,^{1,2} Ronald N. Cortright,^{1,2,8} David H. Wasserman,⁴ and P. Darrell Neuffer^{1,2,8}

¹Metabolic Institute for the Study of Diabetes and Obesity, ²Department of Exercise and Sport Science, and ³Department of Cardiovascular Sciences, East Carolina University, Greenville, North Carolina, USA. ⁴Department of Molecular Physiology and Biophysics, Vanderbilt University, Nashville, Tennessee, USA. ⁵Department of Biology, East Carolina University, Greenville, North Carolina, USA. ⁶Department of Pathology, University of Washington, Seattle, Washington, USA. ⁷Department of Pharmacology, Weill Medical College of Cornell University, New York, New York, USA. ⁸Department of Physiology, East Carolina University, Greenville, North Carolina, USA.

High dietary fat intake leads to insulin resistance in skeletal muscle, and this represents a major risk factor for type 2 diabetes and cardiovascular disease. Mitochondrial dysfunction and oxidative stress have been implicated in the disease process, but the underlying mechanisms are still unknown. Here we show that in skeletal muscle of both rodents and humans, a diet high in fat increases the H₂O₂-emitting potential of mitochondria, shifts the cellular redox environment to a more oxidized state, and decreases the redox-buffering capacity in the absence of any change in mitochondrial respiratory function. Furthermore, we show that attenuating mitochondrial H₂O₂ emission, either by treating rats with a mitochondrial-targeted antioxidant or by genetically engineering the overexpression of catalase in mitochondria of muscle in mice, completely preserves insulin sensitivity despite a high-fat diet. These findings place the etiology of insulin resistance in the context of mitochondrial bioenergetics by demonstrating that mitochondrial H₂O₂ emission serves as both a gauge of energy balance and a regulator of cellular redox environment, linking intracellular metabolic balance to the control of insulin sensitivity.

Introduction

Obesity has become a worldwide epidemic, the consequences of which represent a major health care challenge in the 21st century. A decrease in the sensitivity of skeletal muscle to insulin is one of the earliest maladies associated with obesity, and its persistence is a prominent risk factor for type 2 diabetes and cardiovascular disease. The accumulation of lipid in skeletal muscle has long been associated with the development of insulin resistance (1), a maladaptive response that is currently attributed to the generation and intracellular accumulation of proinflammatory lipid metabolites (e.g., fatty acyl-CoAs, diacylglycerols, and/or ceramides) and associated activation of stress-sensitive serine/threonine kinases that antagonize insulin signaling (2–4). Skeletal muscle of obese individuals is also characterized by profound reductions in mitochondrial function, as evidenced by decreased expression of metabolic genes (5, 6), reduced respiratory capacity (7–9), and mitochondria that are smaller and less abundant (9), leading to speculation that a decrease in the capacity to oxidize fat due to acquired or inherited mitochondrial insufficiency may be an underlying cause of the lipid accumulation and insulin resistance that develops in various metabolic states (10, 11).

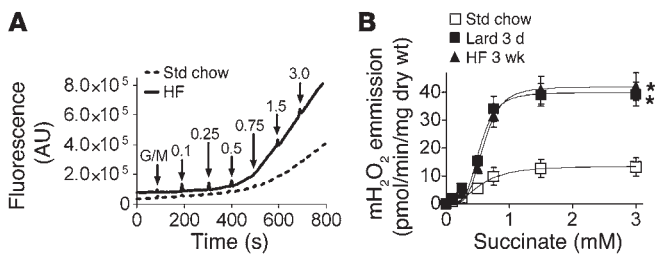
Conflict of interest: A patent application has been filed for the SS peptide technology described in this article. P.D. Neuffer, E.J. Anderson, and H.H. Szeto are the inventors. SS peptide technology is licensed for further research and development to Stealth Peptides Inc., in which H.H. Szeto has financial interests.

Nonstandard abbreviations used: GSH, reduced glutathione; GSH_t, total glutathione; GSSG, oxidized glutathione; HOMA, homeostatic modeling assessment index; MCAT, human catalase targeted specifically to mitochondria.

Citation for this article: *J. Clin. Invest.* 119:573–581 (2009). doi:10.1172/JCI37048.

Oxidative stress has also been implicated in the etiology of insulin resistance associated with type 2 diabetes, based in part on the established role ROS play in the endothelial, renal, and neural complications associated with hyperglycemia in late-stage diabetes (12). Numerous studies have provided indirect evidence of a potential link between oxidative stress and insulin resistance using nonspecific general antioxidant treatments (13–18). More direct evidence was recently provided in cultured adipocytes using a mitochondrial-targeted strategy in which ROS were shown to play a causal role in the development of both TNF- α and glucocorticoid-induced insulin resistance (19). However, the nature and molecular source of ROS, the mechanisms governing production, and its relevance to high-fat diet-induced insulin resistance, the most prevalent form of the disease, remain unknown.

In addition to providing energy for the cell, mitochondria are now recognized as an important site for the generation, dispensation, and removal of a number of intracellular signaling effectors, including hydrogen peroxide (H₂O₂), calcium, and nitric oxide. In fact, the emission rate of H₂O₂ from mitochondria, which reflects the balance between the rate of electron leak/superoxide formation from the respiratory system and scavenging of H₂O₂ in the matrix, varies over a remarkably consistent range across diverse forms of aerobic life (20). Once in the cytosol, H₂O₂ can alter the redox state of the cell by either reacting directly with thiol residues within redox-sensitive proteins or shifting the ratio of reduced glutathione to oxidized glutathione (GSH/GSSG), the main redox buffer of the cell. Thus, the rate at which H₂O₂ is emitted from mitochondria is considered an important barometer of mitochondrial function and modulator of the overall cellular redox environment (21).

**Figure 1**

High-fat diet increases the mitochondrial H₂O₂ emission potential in skeletal muscle. **(A)** Representative trace comparing rates of mitochondrial H₂O₂ emission under state 4 conditions (10 μg/ml oligomycin) in permeabilized skeletal muscle fibers prepared from a red gastrocnemius muscle of rats fed standard chow (Std chow), high-fat diet (HF; lard) for 3 days, or a high-fat (60%) diet for 3 weeks. The experiment was initiated by addition of glutamate/malate (GM, 5 μM/2 μM) to a deenergized fiber bundle (FB), followed by successive additions of succinate (final concentration shown in mM). **(B)** Quantified rates of experiments shown in **A**. Data represent mean ± SEM; *n* = 4, **P* < 0.05 vs. Std chow.

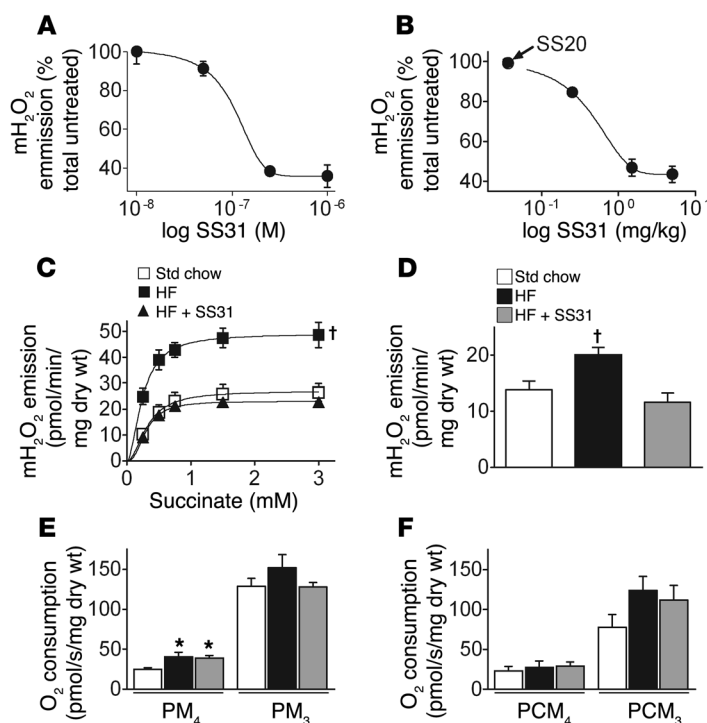
Two recent studies have provided evidence that the rate of mitochondrial H₂O₂ emission is significantly greater when basal respiration is supported by fatty acid- versus carbohydrate-based substrates (22, 23), raising the possibility that mitochondrial H₂O₂ emission may be a primary factor in the etiology of insulin resistance. The purpose of the present study was to more closely examine the potential link between mitochondrial bioenergetics/function and the etiology of high-fat diet-induced insulin resistance in skeletal muscle by (a) determining the influence of both acute and chronic high dietary fat intake on the control of mitochondrial H₂O₂ emission, respiratory function, and overall redox environment in skeletal muscle of both rodents and humans; and (b) determining the impact of novel mitochondrial targeted pharmacological and transgenic antioxidant approaches on insulin sensitivity. Our findings reveal that both acute and chronic high dietary fat intake lead to a dramatic increase in the H₂O₂-emitting potential of mitochondria in the absence of any change in respiratory function, generating a shift to a more oxidized cellular redox environment that, if persistent, leads to the development of insulin resistance in skeletal muscle.

Results

High-fat diet increases mitochondrial H₂O₂-emitting potential. To determine the potential impact of high dietary fat intake on the control of cellular redox balance in skeletal muscle, we used an approach previously developed by our group to measure the rate of mitochondrial H₂O₂ emission in permeabilized skeletal muscle fiber bundles (22, 24). During basal state 4 respiration supported by NADH-linked complex I substrates, the rate of superoxide formation is low, representing 0.1%–0.5% of total O₂ utilization (23, 24). However, respiration supported exclusively by succinate, an FADH₂-linked complex II substrate, elicits high rates of superoxide production by generating reverse electron flow back into complex I (23–26). To provide a better measure of the respiratory system's potential to generate and/or emit H₂O₂ in relation to a progressively increasing supply of reducing equivalents (without a change in ATP demand), we continuously monitored changes in H₂O₂ emission in response to titration of succinate during state 4 respi-

ration supported by the complex I substrates pyruvate and malate. By plotting the rate of H₂O₂ emission versus succinate concentration, we reasoned that a leftward shift in the curve would indicate an increase, whereas a rightward shift would indicate a decrease, in the H₂O₂-emitting potential of the respiratory system. Surprisingly, switching rats from a standard high-carbohydrate chow diet to 100% fat (lard) for 3 days or a 60% high-fat diet for 3 weeks induced a remarkable 3- to 4-fold increase in the maximal rate of mitochondrial H₂O₂ emission, with little to no change in sensitivity (Figure 1, A and B). Addition of rotenone at the conclusion of succinate titration eliminated H₂O₂ emission (data not shown), confirming complex I as the source of superoxide production in both control and high-fat diet-fed rats. Mitochondrial H₂O₂-emitting potential was also assessed by titrating pyruvate/malate in the presence of antimycin A (complex III inhibitor), again revealing a greater than 2-fold-higher maximal rate of H₂O₂ emission in high-fat diet-fed rats (Supplemental Figure 1; supplemental material available online with this article; doi:10.1172/JCI37048DS1). These findings demonstrate that the mitochondrial H₂O₂-emitting potential in skeletal muscle is markedly increased within as few as 3 days after transitioning to a high-fat diet.

SS31 prevents the increase in mitochondrial H₂O₂-emitting potential. To further examine the factors governing mitochondrial H₂O₂ emission in the context of a high-fat diet, we turned to a recently developed cell-permeable small peptide antioxidant, SS31. SS31 is unique in that it localizes specifically within the mitochondrial inner membrane, where it scavenges electrons without affecting membrane potential or respiratory control (27). This small peptide antioxidant has been found to effectively reduce superoxide production in hearts subjected to myocardial stunning (27), in pancreatic islet cells after transplantation (28), and in animal models of Parkinson and amyotrophic lateral sclerosis diseases (29, 30). We initially established in vitro (Figure 2A) and in vivo (Figure 2B) dose-response curves for SS31 under maximal H₂O₂-producing conditions, both of which revealed greater than 50% reduction in mitochondrial H₂O₂ emission when compared with vehicle (saline) and/or SS20 (small peptide without antioxidant properties). Next, we placed rats on a high-fat diet (60%) for 6 weeks with or without daily administration of SS31. Succinate titration experiments conducted on permeabilized fibers again revealed a remarkable, 3-fold increase in the maximal rate of H₂O₂ emission in high-fat diet-fed rats (Figure 2C). Parallel experiments using palmitoylcarnitine plus malate, a more physiological substrate combination, also generated a nearly 2-fold greater rate of H₂O₂ emission in permeabilized fibers from high-fat diet-fed rats (Figure 2D). However, in high-fat diet-fed rats treated with SS31, the increase in mitochondrial H₂O₂-emitting potential during both succinate or palmitoylcarnitine supported respiration was completely prevented (Figure 2, C and D). Basal respiration supported by pyruvate/malate was slightly increased in fibers from high-fat diet-fed rats, suggesting some degree of uncoupling (Figure 2E). However, in high-fat diet-fed rats, basal rates of pyruvate/malate- or palmitoylcarnitine-supported respiration were not affected by SS31 treatment (Figure 2, E and F), indicating that the normalization of H₂O₂ emission with SS31 treatment was not mediated by an increase in proton leak. No evidence of mitochondrial dysfunction (maximal ADP-stimulated respiration; Figure 2, E and F) or oxidative stress, at least with respect to the levels of the lipid peroxide derivative 4-hydroxy-non-enal (data not shown), was found in muscle of high-fat diet-fed rats with or without SS31 treatment. SS31 treatment also had

**Figure 2**

The mitochondrial-targeted antioxidant SS31 prevents the increase in mitochondrial H₂O₂-emitting potential caused by high-fat diet in red gastrocnemius skeletal muscle of rats. (A and B) Dose-response curves for mitochondrial H₂O₂ (mH₂O₂) emission following in vitro or in vivo administration of SS31. (A) Permeabilized fibers were briefly incubated in a range of SS31 concentrations prior to being assayed for maximal H₂O₂ emission under state 4 conditions (5 mM pyruvate/2 mM malate, 10 μg/ml oligomycin) in the presence of the complex III inhibitor antimycin A (10 μM). (B) Permeabilized fibers were assayed for maximal succinate-induced (3 mM) mitochondrial H₂O₂ emission under state 4 conditions (10 μg/ml oligomycin) approximately 2 hours following an acute intraperitoneal injection of SS20 (control peptide, 5 mg/kg) or varied concentrations of SS31. (C and D) SS31 ameliorates the increased mitochondrial H₂O₂ emission caused by high-fat diet. Permeabilized fibers were prepared from rats fed (6 weeks) standard chow, high-fat diet, or high-fat diet with daily SS31 administration, and H₂O₂ emission was measured during state 4 respiration (10 μg/ml oligomycin) supported by (C) succinate (as described in Figure 1) or (D) palmitoylcarnitine (25 μM) and malate (2 mM). (E and F) High-fat diet increases basal respiration with NADH-linked substrates, but SS31 has no effect. Permeabilized fibers were prepared from rats treated as indicated above, and respiration was measured with (E) pyruvate/malate (5 mM/2 mM) or (F) palmitoylcarnitine/malate (25 μM/2 mM) in both basal respiratory state 4 (PM₄, PCM₄) and maximal ADP-stimulated (2 mM) respiratory state 3 (PM₃, PCM₃). Data represent mean ± SEM; *n* = 4–6, **P* < 0.05 vs. Std chow; †*P* < 0.05 vs. Std. chow and SS31-treated.

no effect on weight gain in high-fat diet-fed rats (Supplemental Figure 2). Collectively, these findings demonstrate that administration of a mitochondrial targeted antioxidant is sufficient to prevent or compensate for the increase in mitochondrial H₂O₂-emitting potential induced by a high-fat diet.

High-fat diet shifts cellular redox environment to a more oxidized state. It is increasingly recognized that the intracellular localization and activity of many proteins (e.g., receptors, kinases/phosphatases, transcription factors, etc.) is reversibly controlled by the oxidation status of specific thiol-containing (SH-containing) residues.

GSH, the most abundant redox buffer in cells, participates in maintaining the redox state of many of these sulfur switches as well as the overall reduced environment of the cell. GSH is also reversibly oxidized to GSSG by glutathione peroxidase in the presence of H₂O₂. Thus, the GSH/GSSG ratio is extremely dynamic, reflecting the cellular redox environment, which in turn regulates the biological status of the cell (21, 31). To determine whether the high-fat diet-induced increase in H₂O₂-emitting potential measured in situ is related to changes in the cellular redox environment in vivo, we measured both GSH and GSSG in skeletal muscle of chow-fed and high-fat diet-fed rats under 2 conditions: after a 10-hour fast and 1 hour after administration of a standard glucose load (oral gavage, 10-hour fasted). In chow-fed controls, glucose ingestion elicited an approximately 2-fold increase in GSSG (Figure 3A) and an approximately 50% reduction in the GSH/GSSG ratio (Figure 3B), presumably reflecting an increase in mitochondrial H₂O₂ emission in response to the insulin-stimulated increase in glucose uptake and oxidation. In high-fat diet-fed rats, the GSH/GSSG ratio was already reduced by approximately 50% in the 10-hour fasted state relative to that in chow-fed controls and declined further in response to glucose ingestion (Figure 3B), consistent with a further increase in GSSG (Figure 3A). Interestingly, SS31 treatment completely prevented the acute increase in GSSG and decrease in GSH/GSSG ratio in response to glucose ingestion, providing evidence that the acute change in redox state is indeed mediated by H₂O₂ released by the mitochondria. Nevertheless, total cellular glutathione content (GSH_t) decreased by approximately 30% in high-fat diet-fed rats, irrespective of SS31 treatment (Figure 3C), suggesting that high fat intake compromises total GSH-mediated redox buffering capacity in skeletal muscle.

H₂O₂ emission links mitochondria to insulin sensitivity. To further test whether mitochondrial H₂O₂ emission and/or intracellular redox environment may be linked to the etiology of high-fat diet-induced insulin resistance, we performed oral glucose tolerance tests in rats after the 6-week high-fat diet (Figure 4, A and B). Greater AUCs for both blood glucose and insulin (Figure 4C) and increased homeostatic model assessment index (HOMA; Figure 4D) confirmed the development of insulin resistance in high-fat diet-fed rats. Treatment of high-fat diet-fed rats with SS31 completely blocked the development of insulin resistance (Figure 4, C and D). To further assess insulin sensitivity, we measured the phosphorylation state of the insulin signaling protein Akt in skeletal muscle of animals after a 10-hour fast or 1 hour after they received an oral glucose load. In response to glucose ingestion, Akt phosphorylation increased approximately 5-fold in skeletal muscle of chow-fed controls but was unchanged in high-fat diet-fed rats (Figure 4E and Supplemental Figure 3), confirming the presence of insulin resistance at the level of insulin signaling. Treatment of high-fat diet-fed rats with SS31 completely preserved Akt phosphorylation in response to glucose ingestion, again indicating maintenance of insulin sensitivity.

To specifically determine whether mitochondrial H₂O₂ emission is a primary factor in the development of diet-induced insulin resistance, we studied transgenic C57BL/6J mice overexpressing human catalase targeted specifically to mitochondria in skeletal and cardiac muscle (MCAT mice) (32). Catalase, which is

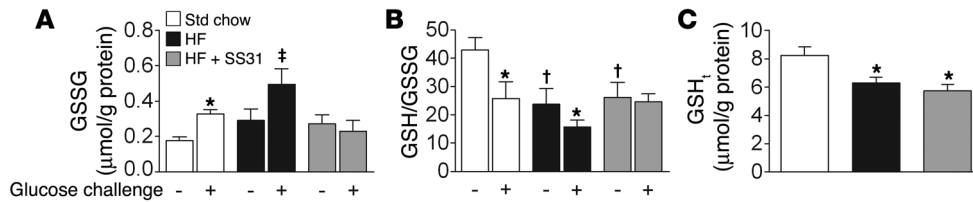


Figure 3

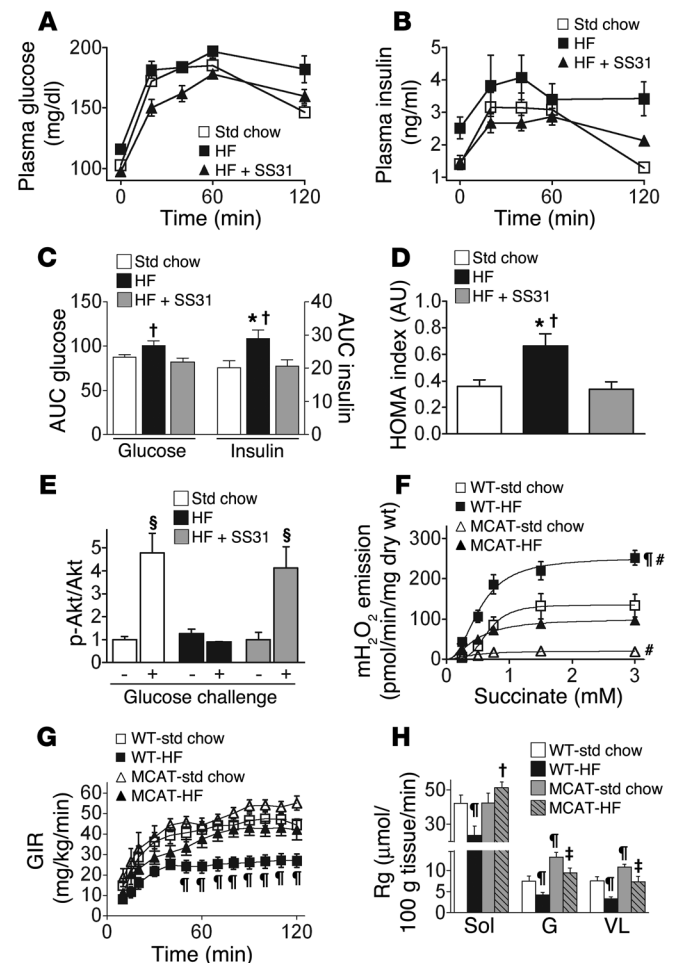
High-fat diet shifts the intracellular redox environment to a more oxidized state in skeletal muscle. (A and B) SS31 prevents the increase in GSSG and decrease in GSH/GSSG ratio in response to acute glucose ingestion. GSSG content (A) and GSH/GSSG ratio (B) were measured before (–) and 1 hour after (+) oral glucose ingestion in red gastrocnemius muscle of rats (10-hour-fasted) fed standard chow, high-fat diet (6 weeks), or high-fat diet with daily SS31 treatment. (C) Muscle GSH_i in standard chow–fed, high-fat diet–fed, and high-fat diet–fed plus SS31-treated rats. Data represent mean ± SEM; n = 4–6, *P < 0.05 vs. corresponding fasted state (i.e., before glucose injection); †P < 0.05 vs. Std chow before glucose injection; ‡P < 0.05 vs. all other groups.

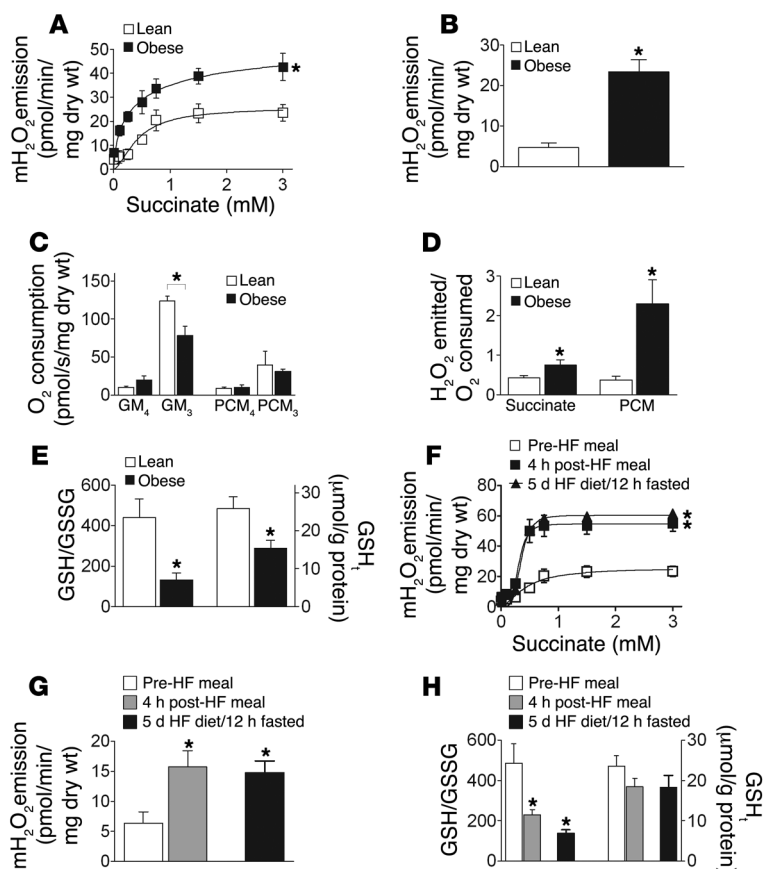
normally localized only in peroxisomes, catalyzes the reduction of H₂O₂ to H₂O. Similar to rats, wild-type littermates maintained on a high-fat diet generated 2.5-fold-higher rates of mitochondrial H₂O₂ emission in response to succinate titration when compared with wild-type mice on a standard chow diet. By contrast, H₂O₂ emission rates in MCAT mice on a high-fat diet were well below rates obtained in wild-type mice on the high-fat diet. H₂O₂ emission rates were lowest in MCAT mice on standard chow (Figure 4F). Similarly, GSH_i, which decreased in wild-type mice on a high-fat diet, was preserved in MCAT mice on the high-fat diet (Supplemental Figure 4). We next performed hyperinsulinemic-euglycemic clamps on MCAT and wild-type mice maintained on either a high-fat or standard chow diet. In high-fat diet–fed mice, mitochondrial targeted catalase activity in muscle preserved both whole-body insulin sensitivity (glucose infusion rate during clamp; Figure 4G) and muscle-specific rates of insulin-stimulated glucose uptake (Figure 4H). These data confirm mitochondria as the source of H₂O₂ and demonstrate that mitochondrial H₂O₂ emission is a primary factor linking high fat intake to the etiology of insulin resistance in skeletal muscle.

Figure 4

Mitochondrial-targeted scavenging of H₂O₂ prevents high-fat diet–induced insulin resistance in skeletal muscle. (A–D) Whole body insulin sensitivity is preserved in high-fat diet–fed rats treated with SS31. (A) Plasma glucose and (B) plasma insulin concentrations in response to oral glucose challenge. (C) AUC (arbitrary units) for both glucose and insulin and (D) HOMA, a fasting index of insulin action. Data represent mean ± SEM; n = 9–10; *P < 0.05 vs. Std chow; †P < 0.05 vs. SS31-treated. (E) Preserved insulin signaling in high-fat diet–fed animals treated with SS31. Phosphorylated Akt relative to total Akt in response to glucose challenge in red gastrocnemius muscle (representative blots shown in Supplemental Figure 2). Data represent mean ± SEM; n = 4–5; §P < 0.05 vs. before glucose challenge. (F–H) Targeted expression of MCAT prevents high-fat diet–induced increase in mitochondrial H₂O₂ emission and insulin resistance in transgenic mice. (F) Succinate stimulated H₂O₂ emission (as described in Figure 1) during state 4 respiration (10 μg/ml oligomycin) in permeabilized red gastrocnemius fibers prepared from wild-type and MCAT mice (4- to 5-hour fasted) fed standard chow or high-fat (60%) diet for 12 weeks. (G) Glucose infusion rate (GIR) during hyperinsulinemic-euglycemic clamps. (H) Rate of glucose uptake (Rg) in soleus (Sol), gastrocnemius (G), and vastus lateralis (VL) skeletal muscle from mice in G. Data represent mean ± SEM; n = 4 for mH₂O₂ and n = 9–11 for glucose-clamp experiments; †P < 0.05 vs. WT–std chow; #P < 0.05 vs. MCAT–HF; ‡P < 0.05 vs. WT–HF and MCAT–std chow.

Obesity/diet alter mitochondrial H₂O₂ emission in humans. To further explore the relationship between mitochondrial H₂O₂ emission and insulin resistance, and to determine whether the same phenomena occur in humans, we measured the control of mitochondrial H₂O₂ emission and respiration in permeabilized skeletal myofiber bundles obtained by muscle biopsy from lean, insulin-sensitive (BMI, 21.6 ± 1.2 kg/m²; HOMA, 1.2 ± 0.4) and obese, insulin-resistant (BMI, 43.0 ± 4.1 kg/m²; HOMA, 2.5 ± 0.7; P < 0.05) male human subjects. Mitochondrial H₂O₂ emission was approxi-



**Figure 5**

Mitochondrial H₂O₂ emission is higher in human obese males and acutely increases in lean males following a high-fat meal. (A and B) Mitochondrial H₂O₂ emission in permeabilized fibers prepared from vastus lateralis of obese and lean human males during state 4 respiration (10 μg/ml oligomycin) supported by (A) succinate (as described in Figure 1) or (B) palmitoylcarnitine (25 μM) and malate (2 mM). (C) O₂ consumption rate determined from parallel experiments during glutamate/malate- or palmitoylcarnitine/malate-supported basal state 4 (GM₄, PCM₄) and maximal ADP-stimulated (2 mM) state 3 (GM₃, PCM₃) respiration. (D) Ratio of H₂O₂ emitted to O₂ consumed under state 4 conditions. (E) GSH/GSSG ratio and GSH_t in skeletal muscle from lean versus obese subjects. (F and G) High-fat diet increases mitochondrial H₂O₂ emission in lean males. Mitochondrial H₂O₂ emission measured during (F) succinate- and (G) palmitoylcarnitine-supported state 4 respiration (10 μg/ml oligomycin) in permeabilized fibers prepared from lean males before (10-hour fasted) and 4 hours after a high-fat meal and after 5 days on a high-fat diet (10-hour fasted). (H) GSH/GSSG ratio and muscle GSH_t in lean males in response to both acute and 5-day lipid ingestion. Data represent mean ± SEM; *n* = 5–9; **P* < 0.05 vs. lean or fasted male (control) for that respective experiment.

mately 2-fold higher in obese versus lean individuals in response to titration of succinate (Figure 5A) and nearly 4-fold higher during basal respiration supported by fatty acid (Figure 5B). Despite the difference in H₂O₂ emission, the basal O₂ utilization rate was similar in lean and obese subjects (Figure 5C); consequently, the rate of mitochondrial free radical leak was approximately 2-fold higher during glutamate/malate/succinate-supported and greater than 4-fold higher during palmitoylcarnitine-supported basal respiration (Figure 5D). Maximal ADP-stimulated O₂ consumption was approximately 35% lower in permeabilized myofibers from the obese subjects (Figure 5C), consistent with the reduced respiratory capacity and mitochondrial content previously reported in muscle of obese individuals (9). As was observed in rodents fed a high-fat diet (Figure 3 and Supplemental Figure 4), both cellular GSH_t and the GSH/GSSG ratio were approximately 50% lower in skeletal muscle of obese humans (Figure 5E). For the subjects as a group, the GSH/GSSG ratio was negatively correlated with both BMI and HOMA (Supplemental Figure 5), providing evidence that shifts in intracellular redox environment reflect the overall metabolic status of cells.

To determine whether excess dietary lipid intake can acutely affect mitochondrial H₂O₂ emission in lean, insulin-sensitive humans, muscle biopsies were obtained from lean (BMI, 20–25 kg/m²) male subjects before (12-hour fasted) and 4 hours after consumption of a high-fat meal (35% of daily energy expenditure; 60%–65% fat), and after 5 days of consumption of a similar high-fat diet (12-hour fasted). Remarkably, within 4 hours after consumption of a high-fat meal, maximal mitochondrial H₂O₂

emission was increased by more than 2-fold in response to succinate titration (Figure 5F) and during state 4 respiration supported by palmitoylcarnitine plus malate (Figure 5G). Moreover, this heightened mitochondrial H₂O₂-emitting potential persisted through the 5-day high-fat diet regimen. Cellular GSH/GSSG ratio decreased by approximately 50% within 4 hours after consumption of the high-fat meal and remained at this level through the 5-day high-fat diet (Figure 5H), again indicative of a shift in redox environment to a more oxidized state. Total cellular GSH content did not significantly change (Figure 5H). These findings demonstrate that the factors governing mitochondrial H₂O₂ emission and the cellular redox environment in skeletal muscle are remarkably sensitive to dietary lipid intake.

Discussion

Although excess lipid accumulation has long been associated with the development of insulin resistance in skeletal muscle (33, 34), more recent research has provided evidence that oxidative stress may be a major determining factor in the loss of both insulin sensitivity and mitochondrial function associated with high dietary fat intake and obesity (13, 19). However, oxidative stress itself is a rather vague concept, typically viewed as the consequence of an imbalance between pro-oxidants and antioxidants sufficient to cause oxidative modification/damage of macromolecules. In the much broader context of redox systems biology, redox signaling mechanisms function well below the threshold of “oxidative stress” and are critical to maintaining cellular homeostasis (31, 35). In this context, there are 3 main findings from the present study. First, our



results establish mitochondrial H_2O_2 emission and the resulting shift to a more oxidized redox environment, in the absence of any evidence of mitochondrial dysfunction, as an underlying cause of high-fat diet-induced insulin resistance in skeletal muscle. This is supported by experiments that utilized a mitochondrial-targeted small peptide antioxidant in rats and a muscle-specific mitochondrial-targeted H_2O_2 scavenger in transgenic mice, both of which completely prevented the development of insulin resistance with high-fat feeding. Second, our findings reveal that the muscle redox environment, as reflected by both the GSH/GSSG ratio and GSH_t , is remarkably sensitive to nutritional intake, shifting to a more oxidized state in response to both acute (e.g., glucose ingestion) and chronic (e.g., high-fat diet) food ingestion. These data are consistent with the fact that cytosolic GSH is the primary redox buffer for H_2O_2 emitted from mitochondria. Third, high dietary fat intake also increases the maximal H_2O_2 -emitting potential of mitochondria in skeletal muscle, providing evidence of a fundamental change in either the governance of the rate of electron leak from the electron transport system or the rate of H_2O_2 scavenging in the mitochondrial matrix. Together these findings provide strong evidence that mitochondrial H_2O_2 is a critical factor in the etiology of high-fat diet-induced insulin resistance and that its production and emission serve as both a gauge of energy balance (i.e., reducing potential of the electron transport system) and regulator of redox state within myofibers, ultimately linking cellular metabolic balance to the control of insulin sensitivity.

The present study places the etiology of high-fat diet/obesity-induced insulin resistance in the context of mitochondrial bioenergetics; that is, on the mechanisms governing electron flux through, and electron leak from, the respiratory system. Cellular respiration is generally regarded as a demand-driven process, meaning that the rate of electron flux through the electron transport system, and thus oxygen consumption, is determined by the rate at which protons reenter the mitochondrial matrix due to leak through the inner membrane (e.g., basal respiration) or flux through the ATP synthase enzyme, the latter largely governed by the rate of cellular ATP utilization. When cells are in metabolic balance, substrate uptake and catabolism rates through the metabolic pathways are matched to energy demand, ensuring that reducing equivalents (i.e., NADH, $FADH_2$) are provided at a rate sufficient to support respiratory demand. However, mounting evidence suggests that when cells are out of metabolic balance, the oversupply of substrates has a demonstrable impact on cell function. Koves et al. (36) have recently reported the presence of ketone bodies and the accumulation of partially oxidized fatty acids in skeletal muscle of rats fed a high-fat diet, implying that an oversupply of lipids overwhelms the β -oxidation and TCA cycle pathways, generating metabolic intermediates that otherwise are not present. The generation of surplus reducing equivalents would in turn be expected to elevate the redox state of complex I and/or the ubiquinone pool. Under resting conditions, the rate of electron leak from complex I is extremely sensitive to redox state/membrane potential (37–40), such that even a small surplus of reducing equivalents would be predicted to elicit an exponential increase in the rate of superoxide production and H_2O_2 emission from mitochondria. In the present study, we observed a near doubling of GSSG and approximately 50% reduction in GSH/GSSG ratio in muscle of both control and high-fat diet-fed rats within 1 hour after oral glucose gavage (Figure 3, A and B). This is consistent with insulin stimulating glucose uptake and flux through metabolism, generating an increase in

mitochondrial H_2O_2 emission that is in turn buffered by GSH. The response to carbohydrate ingestion, however, is likely transient, owing to the rapid clearance of glucose. By contrast, a diet high in fat generated a persistent reduction in GSH/GSSG (i.e., evident even after 12-hour fast; Figure 3B and Figure 5, E and H), suggesting that the clearance and metabolism of dietary lipids may elicit a more sustained elevation in H_2O_2 emission, shifting the cellular redox environment to a more persistent oxidized state.

At least 3 additional factors may be contributing to a more oxidized redox environment when skeletal muscle is under lipid overload. The marked increase in the maximal H_2O_2 -emitting potential of the mitochondria in permeabilized fibers, even within 4 hours after consumption of a high-fat meal, is particularly striking. Increased mitochondrial H_2O_2 emission could occur as a result of an increased rate of superoxide production, a decreased rate of H_2O_2 scavenging in the matrix, or a combination of both. A more oxidized redox environment does lead to glutathionylation and/or nitrosation of protein thiols within complex I of the respiratory chain, both of which accelerate electron leak from complex I (41, 42). Interestingly, both redox modifications of complex I require a significant portion of the mitochondrial GSH pool to be oxidized and are readily reversed by restoration of GSH/GSSG ratios, providing further evidence of regulation exerted by reversible redox modification (43, 44). A second factor may be related to mitochondrial morphology. In skeletal muscle, mitochondria exist as an interconnected reticular network that is thought to facilitate transmission of membrane potential as well as the distribution of antioxidant activities (45). Increased mitochondrial ROS generation induces rapid fission of the reticulum (46) and, in cells exposed to high glucose, accelerates mitochondrial ROS emission (47). A decrease in the total redox buffer capacity within the cytosol and/or mitochondria is a third potential factor contributing to a shift to a more oxidized redox environment. Although mitochondrial-specific GSH is difficult to measure, GSH_t was significantly lower in muscle of high-fat diet-fed rodents and obese humans (Figure 3B, Figure 5E, and Supplemental Figure 4), likely reflecting loss from the cytosol as well as various subcellular compartments. Both synthesis of GSH and efflux of GSSG from cells are acutely influenced by several factors in addition to H_2O_2 , including nitric oxide and fatty acids (21), potentially explaining why SS31 failed to protect against the diet-induced loss of GSH_t . Nevertheless, these findings raise the intriguing possibility that postprandial mitochondrial H_2O_2 emission may be a key factor in the development of insulin resistance associated with high-fat diets.

Research conducted over the past decade has demonstrated that both obesity and aging are associated with reduced mitochondrial function in skeletal muscle in conjunction with lower whole-body insulin sensitivity (9, 48, 49). In view of the evidence also supporting a link between excess lipid accumulation and insulin resistance in muscle (2, 3), a popular theory emerged to suggest that acquired or inherited mitochondrial dysfunction limits the capacity to oxidize fats in skeletal muscle and thus represents the mechanism underlying the accumulation of lipid metabolites and the development of insulin resistance (10, 11). This interpretation, however, is incompatible with the principles of mitochondrial bioenergetics in that the rate of oxidative metabolism within any cell is determined by (a) the rate of proton leak across the inner membrane and (b) the rate of ATP utilization, the capacity for which greatly exceeds substrate oxidation rates measured at rest (particularly in skeletal muscle). Thus, the intracellular accumulation of lipid metabolites more



likely reflects the simple consequence of fatty acid supply exceeding metabolic demand, regardless of mitochondrial content. In fact, transitioning to a high-fat diet initially induces an increase, not a decrease, in mitochondrial biogenesis and fatty acid oxidative capacity in skeletal muscle (50, 51), presumably as an adaptive response to the elevated lipid load. Moreover, Bonnard et al. (13) recently reported that deteriorations in mitochondrial structure and function in skeletal muscle of mice appear only after several months of high-fat feeding, well after insulin resistance has developed. The implication is that mitochondrial dysfunction, similar to insulin resistance, is a consequence rather than a primary cause of the altered cellular metabolism that develops with nutritional overload (13).

The results of the present study suggest that the biological status of skeletal myofibers, including the degree of insulin sensitivity, is functionally linked to the redox state of the cell. With this mechanism, the reducing potential of the electron transport system provides a means for the cell to sense metabolic imbalance, while the emission of H_2O_2 from the mitochondria provides a means of initiating an appropriate counterbalance response – shifting the redox state and decreasing insulin sensitivity in an attempt to restore metabolic balance. The generation of surplus-reducing equivalents appears to be the critical factor, as transgenic mice engineered to increase flux through β -oxidation specifically in muscle develop severe insulin resistance despite being protected from high-fat diet-induced obesity (52), whereas mice with limited β -oxidative capacity in muscle maintain normal insulin sensitivity on a high-fat diet despite lipid accumulation in muscle and the development of obesity (52, 53). A number of stress-sensitive signaling kinases that target and disrupt IRS-1 signaling, most notably NF- κ B/I κ B/IKK β , are activated by shifting to a more oxidized redox environment (54). Blocking the NF- κ B pathway, either pharmacologically or genetically, has been shown to protect against high-fat diet-induced insulin resistance (55). However, further work will be required to identify the redox-sensitive signaling mechanisms affecting insulin sensitivity.

Linking mitochondrial bioenergetics to the etiology of insulin resistance has a number of clinical implications. First, it is important to recognize that pharmacological approaches designed to improve insulin-stimulated glucose uptake without a corresponding increase in metabolic demand may exacerbate the underlying problem, pushing the intracellular redox environment further toward an oxidized state. Second, the present study demonstrates that the use of a mitochondrial-targeted antioxidant represents a potentially effective counterbalance strategy for treating insulin resistance and other diseases associated with chronic metabolic imbalance. It is worth noting that recent studies using general antioxidant therapeutics for the prevention and treatment of insulin resistance have led to disappointing and even contradictory results (56–58). Thus, the development of an antioxidant targeted specifically to mitochondria is an important experimental advance that could have important therapeutic implications. Third, relieving the reducing potential through introduction of a mitochondrial uncoupler represents an alternative approach, although the degree of uncoupling must be carefully controlled to avoid excessive heat production (59). Finally, linking mitochondrial bioenergetics to insulin sensitivity provides a mechanistic basis for the clinical strategies that have proven most effective in treating obesity-induced insulin resistance and type 2 diabetes; i.e., simply reestablishing cellular metabolic balance by limiting caloric intake and/or increasing metabolic demand through increased physical activity.

Methods

Materials, reagents, animals, and diet. Amplex Red Ultra reagent was obtained from Invitrogen. HRP and methyl-2-vinylpyridinium triflate were obtained from Fluka Biochemika (Sigma-Aldrich), and all other chemicals were purchased from Sigma-Aldrich. Antibodies for Akt and phospho-Akt were obtained from Cell Signaling Technology. All animal studies were approved by the East Carolina University Institutional Animal Care and Use Committee. Male Sprague-Dawley rats (8 weeks old) were obtained from Charles River Laboratory. Heterozygous MCAT mice were maintained on the C57BL/6 background as originally described (32). All rodents were housed in a temperature- (22°C) and light-controlled (12-hour light/12-hour dark) room and maintained on either standard rodent chow or a high-fat (60%) diet (Research Diets), with free access to food and water. At the conclusion of the study, rats were fasted 10 hours, anesthetized (100 mg/kg ketamine/xylazine, intraperitoneally), and red portions of the gastrocnemius muscle were dissected for preparation of permeabilized muscle fibers (10 mg) or frozen for later analysis.

SS31 administration. Some high-fat diet-fed rats received daily intraperitoneal injections of SS31 dissolved in PBS (1.5 mg/kg). Initial in vitro and in vivo SS31 dose-response studies were conducted with a control peptide, SS20, that lacks the free radical scavenging properties. No difference in H_2O_2 emission was observed between vehicle- and SS20-treated rats (Figure 2B). Therefore, all subsequent 6-week treatment studies used only SS31.

Oral glucose tolerance tests. On the day of experiments, food was removed 10 hours prior to administration of a 2 g/kg glucose solution via gavage. Glucose levels were determined on whole blood samples (LifeScan). Serum insulin levels were determined via a rat/mouse ELISA kit (Linco; Millipore). Fasting data were used to determine HOMA, calculated as fasting insulin (μ U/ml) \times fasting glucose (mM)/22.5.

Preparation of permeabilized muscle fiber bundles. This technique is partially adapted from previous methods (60, 61) and has been thoroughly described (22, 24). In brief, samples of muscle were placed in ice-cold buffer X, containing (in mM) 60 K-MES, 35 KCl, 7.23 K_2 EGTA, 2.77 CaK_2 EGTA, 20 imidazole, 0.5 DTT, 20 taurine, 5.7 ATP, 15 PCr, 6.56 $MgCl_2 \cdot 6H_2O$ (pH 7.1, 295 mOsm) and trimmed of connective tissue and fat; small bundles of fibers were prepared and gently separated along their longitudinal axis. Fiber bundles were then treated with 50 μ g/ml saponin, a mild, cholesterol-specific detergent that selectively permeabilizes the sarcolemmal membranes while keeping mitochondrial membranes (which lack significant levels of cholesterol) completely intact. Following permeabilization, the permeabilized fiber bundles were washed in ice-cold buffer Z containing (in mM) 110 K-MES, 35 KCl, 1 EGTA, 5 K_2HPO_4 , 3 $MgCl_2 \cdot 6H_2O$, 5 mg/ml BSA, 0.05 pyruvate, and 0.02 malate (pH 7.4, 295 mOsm) and remained in buffer Z on a rotator at 4°C until analysis (<2 hours).

Mitochondrial respiration and H_2O_2 emission measurements. High-resolution O_2 consumption measurements were conducted at 30°C in buffer Z using the OROBOROS O_2K Oxygraph. Mitochondrial H_2O_2 emission was measured in buffer Z at 30°C during state 4 respiration (10 μ g/ml oligomycin) by continuously monitoring oxidation of Amplex Red using a SPEX Fluoromax 3 (HORIBA Jobin Yvon) spectrofluorometer with temperature control and magnetic stirring at more than 1,000 rpm. For respiration measurements, 50 μ M benzyltoluene sulfonamide (BTS) was included in buffer Z. BTS is a potent inhibitor of contraction of both intact and permeabilized muscle fibers (62) and has been found to dramatically stabilize and improve the responsiveness of permeabilized fiber bundles during respiratory measurements (D.A. Kane, E.J. Anderson, C.-T. Lin, C.G.R. Perry, and P.D. Neuffer, unpublished observations). For mitochondrial H_2O_2 emission measurements (state 4), fiber bundles were briefly incubated in 10 mM pyrophosphate prior to assay to deplete fibers of all endogenous adenine nucleotides and to inhibit contraction of the fibers during the assay. At



the conclusion of each experiment, permeabilized fibers were washed in double-distilled H₂O to remove salts and freeze-dried in a lyophilizer (Lab-conco). The rate of respiration is expressed as pmol/s/mg dry weight and mitochondrial H₂O₂ emission expressed as pmol/min/mg dry weight.

Preparation of muscle protein. Gastrocnemius (rat) and vastus lateralis (human) muscle samples were frozen in liquid N₂ and powdered by pulverization. To prepare samples for GSH measurement, we added approximately 100 mg of tissue to a test tube containing (in mM): 10 Tris, 1 EDTA, 1 EGTA, 2 Na-orthovanadate, 2 Na-pyrophosphate, 5 NaF, protease inhibitor cocktail (Complete; Roche Diagnostics) at pH 7.2. This tissue suspension was then homogenized on ice 3 times for 10 seconds each, using a Polytron SC-250 set at 25,000 rpm. After homogenization, 1% Triton X-100 was added to the protein suspension, vortexed, and allowed to sit on ice for 5 minutes. The tubes were then spun at 13,000 g for 10 minutes to pellet the insoluble debris. For GSSG measurement, 100 mg of tissue was added to a test tube containing the above reagents plus 1 mM methyl-2-vinylpyridinium triflate to scavenge all reduced thiols in the sample. The tissue was then homogenized as above, incubated at room temperature for 5 minutes, and then spun at 13,000 g as above.

GSH and GSSG measurements. For GSSG measurement, tissue was homogenized in a solution containing 1 mM methyl-2-vinylpyridinium triflate to scavenge all reduced thiols in the sample. Total GSH and GSSG were then measured using the reagents and calibration set provided by the GSH/GSSG assay (Oxis International Inc.) according to the manufacturer's instructions, with small modifications as needed.

Hyperinsulinemic, euglycemic clamps. Procedures were approved by the Vanderbilt Animal Care and Use Committee. Mice were catheterized at least 5 days prior to experimentation. Mice were anesthetized with sodium pentobarbital (70 mg/kg body weight). The left common carotid artery was catheterized for sampling with a 2-part catheter consisting of PE-10 (inserted into the artery) and Silastic (outer diameter [OD], 0.025). The right jugular vein was catheterized for infusions with a silastic catheter (OD, 0.025). The free catheter ends were tunneled under the skin to the back of the neck and attached via stainless steel connectors to tubing made of Micro-Renathane (OD, 0.033), which were externalized and sealed with stainless steel plugs. Lines were flushed daily with approximately 50 µl saline containing 200 U/ml heparin and 5 mg/ml ampicillin. Animals were individually housed after surgery, and body weight was recorded daily. Any mouse not within 10% of presurgery weight by postsurgery day 5 was excluded. Mice fasted for 5 hours were studied in individual 1.4-l plastic containers with bedding or a restrainer (552-BSRR; Plas Labs Inc.) for cut-tail sampling.

The insulin clamp protocol consisted of a 120-minute tracer equilibration period ($t = -120$ to 0 minutes) beginning at 8:00 a.m. followed by a 120-minute experimental period ($t = 0$ -120 minutes) beginning at 10:00 a.m. A blood sample (~5 µl) was obtained at $t = -120$ minutes to determine initial glucose levels (HemoCue meter). At $t = -5$ minutes, a blood sample (~100 µl) was taken for assessment of basal glucose and insulin levels. The insulin clamp was begun at $t = 0$ minutes with a primed-continuous infusion of human insulin (bolus of 16 mU/kg, followed by 4.0 mU/kg/min; Humulin R; Eli Lilly). Euglycemia (~150 mg/dl) was maintained during clamps by measuring blood glucose every 10 minutes starting at $t = 0$ minutes and infusing 50% dextrose as necessary. A 12 µCi bolus of 2[¹⁴C]deoxyglucose (2[¹⁴C]DG) was given at $t = 78$ minutes. Blood samples (80-240 µl) were taken every 10 minutes from $t = 80$ to $t = 120$ minutes and processed to determine plasma 2[¹⁴C]DG levels. Clamp insulin was determined at

$t = 100$ and $t = 120$ min. Mice received saline-washed erythrocytes from donors throughout the experimental period (5-6 µl/minutes) to prevent a fall of more than 5% hematocrit. At $t = 120$ minutes, mice were anesthetized with sodium pentobarbital and tissues were excised, immediately frozen, and stored at -80°C until analysis.

Human subjects and tissue biopsy. Eight healthy men (aged 18-31 years) of a variety of races were recruited to participate in this investigation; 5 were classified as lean (BMI, 21.6 ± 1.2 kg/m²) and 3 were classified as morbidly obese (BMI, 43.0 ± 4.1 k/m²). All participants were nonsmokers with no history of metabolic disease. None of the subjects had any diseases or were taking any medications known to alter metabolism. The subjects were given both oral and written information about the experimental procedures before giving their informed consent. The experiments were approved by the Institutional Review Board of East Carolina University and conducted in accordance with the Declaration of Helsinki principles.

On the day of the experiment, subjects reported to the laboratory following an overnight fast (approximately 12 hours). A fasting blood sample was obtained for determination of glucose and insulin (LabCorp). Height and body weight were recorded, and skeletal muscle biopsies were obtained from the lateral aspect of the vastus lateralis by the percutaneous needle biopsy technique under local subcutaneous anesthesia (1% lidocaine). A portion of each biopsy sample was flash frozen in liquid N₂ for protein analysis and another portion used to prepare permeabilized fiber bundles. Nine healthy lean (BMI, <25 kg/m²) men (aged 18-25 years) of a variety of races participated in an acute high-fat diet study. Subjects reported to the laboratory following a 12-hour overnight fast. After muscle samples were obtained, subjects consumed a single high-fat meal (35% daily kcal intake; >60% kcal from fat), and a second muscle biopsy was taken 4 hours later. Subjects then consumed a high-fat diet (isocaloric; >60% kcal from fat) for 5 days and returned 12-hour fasted on the morning of the sixth day, when a final muscle biopsy was obtained.

Statistics. Data are presented as mean ± SEM. Statistical analyses were performed using 1-way or 2-way ANOVA (as appropriate) with Student-Newman-Keuls method for analysis of significance among groups. The level of significance was set at $P < 0.05$.

Acknowledgments

The authors thank the subjects that participated in this study and J. Patrick Canham for subject recruitment. E.J. Anderson and P.D. Neuffer also thank James I. Elliot and Margaret M. Elliot, Keck Foundation Biotechnology Resource Laboratory, Yale University, for assistance with the initial SS peptide synthesis. This work was supported in part by NIH grants AG001751 (to P.S. Rabinovitch), DK056112 (to J.A. Houmard), DK075880 (to R.N. Cortright), DK54902 (to D.H. Wasserman), DK59637 (to the Vanderbilt Mouse Metabolic Phenotyping Center), and DK073488 (to P.D. Neuffer).

Received for publication August 5, 2008, and accepted in revised form December 10, 2008.

Address correspondence to: P. Darrell Neuffer, Department of Physiology, 6N98, Brody School of Medicine, East Carolina University, Greenville, North Carolina 27834, USA. Phone: (252) 744-2780; Fax: (252) 744-3460; E-mail: neufferp@ecu.edu.

1. McGarry, J.D. 2002. Banting lecture 2001: dysregulation of fatty acid metabolism in the etiology of type 2 diabetes. *Diabetes*. **51**:7-18.
 2. Wellen, K.E., and Hotamisligil, G.S. 2005. Inflammation, stress, and diabetes. *J. Clin. Invest.*

115:1111-1119.
 3. Holland, W.L., and Summers, S.A. 2008. Sphingolipids, insulin resistance, and metabolic disease: new insights from in vivo manipulation of sphingolipid metabolism. *Endocr. Rev.* **29**:381-402.

4. Muoio, D.M., and Newgard, C.B. 2006. Obesity-related derangements in metabolic regulation. *Annu. Rev. Biochem.* **75**:367-401.
 5. Mootha, V.K., et al. 2003. PGC-1alpha-responsive genes involved in oxidative phosphorylation are



- coordinately downregulated in human diabetes. *Nat. Genet.* **34**:267–273.
6. Patti, M.E., et al. 2003. Coordinated reduction of genes of oxidative metabolism in humans with insulin resistance and diabetes: potential role of PGC1 and NRF1. *Proc. Natl. Acad. Sci. U. S. A.* **100**:8466–8471.
7. Boushel, R., et al. 2007. Patients with type 2 diabetes have normal mitochondrial function in skeletal muscle. *Diabetologia.* **50**:790–796.
8. Mogensen, M., et al. 2007. Mitochondrial respiration is decreased in skeletal muscle of patients with type 2 diabetes. *Diabetes.* **56**:1592–1599.
9. Ritov, V.B., et al. 2005. Deficiency of subsarcolemmal mitochondria in obesity and type 2 diabetes. *Diabetes.* **54**:8–14.
10. Lowell, B.B., and Shulman, G.I. 2005. Mitochondrial dysfunction and type 2 diabetes. *Science.* **307**:384–387.
11. Morino, K., Petersen, K.F., and Shulman, G.I. 2006. Molecular mechanisms of insulin resistance in humans and their potential links with mitochondrial dysfunction. *Diabetes.* **55**(Suppl. 2):S9–S15.
12. Evans, J.L., Goldfine, I.D., Maddux, B.A., and Grodsky, G.M. 2002. Oxidative stress and stress-activated signaling pathways: a unifying hypothesis of type 2 diabetes. *Endocr. Rev.* **23**:599–622.
13. Bonnard, C., et al. 2008. Mitochondrial dysfunction results from oxidative stress in the skeletal muscle of diet-induced insulin-resistant mice. *J. Clin. Invest.* **118**:789–800.
14. Evans, J.L., Maddux, B.A., and Goldfine, I.D. 2005. The molecular basis for oxidative stress-induced insulin resistances. *Antioxid. Redox Signal.* **7**:1040–1052.
15. Maddux, B.A., et al. 2001. Protection against oxidative stress – induced insulin resistance in rat L6 muscle cells by micromolar concentrations of {alpha}-lipoic acid. *Diabetes.* **50**:404–410.
16. Rudich, A., Tirosh, A., Potashnik, R., Khamaisi, M., and Bashan, N. 1999. Lipoic acid protects against oxidative stress induced impairment in insulin stimulation of protein kinase B and glucose transport in 3T3-L1 adipocytes. *Diabetologia.* **42**:949–957.
17. Saengsirisuwan, V., Kinnick, T.R., Schmit, M.B., and Henriksen, E.J. 2001. Interactions of exercise training and lipoic acid on skeletal muscle glucose transport in obese Zucker rats. *J. Appl. Physiol.* **91**:145–153.
18. Saengsirisuwan, V., Perez, F.R., Sloniger, J.A., Maier, T., and Henriksen, E.J. 2004. Interactions of exercise training and {alpha}-lipoic acid on insulin signaling in skeletal muscle of obese Zucker rats. *Am. J. Physiol. Endocrinol. Metab.* **287**:E529–E536.
19. Houstis, N., Rosen, E.D., and Lander, E.S. 2006. Reactive oxygen species have a causal role in multiple forms of insulin resistance. *Nature.* **440**:944–948.
20. Stone, J.R., and Yang, S. 2006. Hydrogen peroxide: a signaling messenger. *Antioxid. Redox Signal.* **8**:243–270.
21. Schafer, F.Q., and Buettner, G.R. 2001. Redox environment of the cell as viewed through the redox state of the glutathione disulfide/glutathione couple. *Free Radic. Biol. Med.* **30**:1191–1212.
22. Anderson, E.J., Yamazaki, H., and Neuffer, P.D. 2007. Induction of endogenous uncoupling protein 3 suppresses mitochondrial oxidant emission during fatty acid-supported respiration. *J. Biol. Chem.* **282**:31257–31266.
23. St-Pierre, J., Buckingham, J.A., Roeback, S.J., and Brand, M.D. 2002. Topology of superoxide production from different sites in the mitochondrial electron transport chain. *J. Biol. Chem.* **277**:44784–44790.
24. Anderson, E.J., and Neuffer, P.D. 2006. Type II skeletal myofibers possess unique properties that potentiate mitochondrial H(2)O(2) generation. *Am. J. Physiol. Cell Physiol.* **290**:C844–C851.
25. Liu, Y., Fiskum, G., and Schubert, D. 2002. Generation of reactive oxygen species by the mitochondrial electron transport chain. *J. Neurochem.* **80**:780–787.
26. Turrens, J.F., and Boveris, A. 1980. Generation of superoxide anion by the NADH dehydrogenase of bovine heart mitochondria. *Biochem. J.* **191**:421–427.
27. Zhao, K., et al. 2004. Cell-permeable peptide antioxidants targeted to inner mitochondrial membrane inhibit mitochondrial swelling, oxidative cell death, and reperfusion injury. *J. Biol. Chem.* **279**:34682–34690.
28. Thomas, D., et al. 2005. Mitochondrial targeting to prevent islet cell apoptosis. *J. Am. Soc. Nephrol.* **18**:213–222.
29. Petri, S., et al. 2006. Cell-permeable peptide antioxidants as a novel therapeutic approach in a mouse model of amyotrophic lateral sclerosis. *J. Neurochem.* **98**:1141–1148.
30. Szeto, H.H. 2006. Mitochondria-targeted peptide antioxidants: novel neuroprotective agents. *AAPS J.* **8**:E521–E531.
31. Jones, D.P. 2008. Radical-free biology of oxidative stress. *Am. J. Physiol. Cell Physiol.* **295**:C849–C868.
32. Schriener, S.E., et al. 2005. Extension of murine life span by overexpression of catalase targeted to mitochondria. *Science.* **308**:1909–1911.
33. Hegarty, B.D., Furler, S.M., Ye, J., Cooney, G.J., and Kraegen, E.W. 2003. The role of intramuscular lipid in insulin resistance. *Acta Physiol. Scand.* **178**:373–383.
34. McGarry, J.D. 1992. What if Minkowski had been agnostic? An alternative angle on diabetes. *Science.* **258**:766–770.
35. Jones, D.P. 2006. Disruption of mitochondrial redox circuitry in oxidative stress. *Chem. Biol. Interact.* **163**:38–53.
36. Koves, T.R., et al. 2005. Peroxisome proliferator-activated receptor-gamma co-activator 1alpha-mediated metabolic remodeling of skeletal myocytes mimics exercise training and reverses lipid-induced mitochondrial inefficiency. *J. Biol. Chem.* **280**:33588–33598.
37. Korshunov, S.S., Skulachev, V.P., and Starkov, A.A. 1997. High protonic potential actuates a mechanism of production of reactive oxygen species in mitochondria. *FEBS Lett.* **416**:15–18.
38. Liu, S.S. 1999. Cooperation of a “reactive oxygen cycle” with the Q cycle and the proton cycle in the respiratory chain – superoxide generating and cycling mechanisms in mitochondria. *J. Bioenerg. Biomembr.* **31**:367–376.
39. Liu, S.S. 1997. Generating, partitioning, targeting and functioning of superoxide in mitochondria. *Biosci. Rep.* **17**:259–272.
40. Lee, I., Bender, E., and Kadenbach, B. 2002. Control of mitochondrial membrane potential and ROS formation by reversible phosphorylation of cytochrome c oxidase. *Mol. Cell. Biochem.* **234–235**:63–70.
41. Dahm, C.C., Moore, K., and Murphy, M.P. 2006. Persistent S-nitrosation of complex I and other mitochondrial membrane proteins by S-Nitrosothiols but not nitric oxide or peroxynitrite: implications for the interaction of nitric oxide with mitochondria. *J. Biol. Chem.* **281**:10056–10065.
42. Taylor, E.R., et al. 2003. Reversible glutathionylation of complex I increases mitochondrial superoxide formation. *J. Biol. Chem.* **278**:19603–19610.
43. Dalle-Donne, I., Rossi, R., Giustarini, D., Colombo, R., and Milzani, A. 2007. S-glutathionylation in protein redox regulation. *Free Radic. Biol. Med.* **43**:883–898.
44. Hurd, T.R., Prime, T.A., Harbour, M.E., Lilley, K.S., and Murphy, M.P. 2007. Detection of reactive oxygen species-sensitive thiol proteins by redox difference gel electrophoresis: implications for mitochondrial redox signaling. *J. Biol. Chem.* **282**:22040–22051.
45. Skulachev, V.P. 2001. Mitochondrial filaments and clusters as intracellular power-transmitting cables. *Trends Biochem. Sci.* **26**:23–29.
46. Pletjushkina, O.Y., et al. 2006. Effect of oxidative stress on dynamics of mitochondrial reticulum. *Biochim. Biophys. Acta.* **1757**:518–524.
47. Yu, T., Robotham, J.L., and Yoon, Y. 2006. Increased production of reactive oxygen species in hyperglycemic conditions requires dynamic change of mitochondrial morphology. *Proc. Natl. Acad. Sci. U. S. A.* **103**:2653–2658.
48. Kelley, D.E., He, J., Menshikova, E.V., and Ritov, V.B. 2002. Dysfunction of mitochondria in human skeletal muscle in type 2 diabetes. *Diabetes.* **51**:2944–2950.
49. Petersen, K.F., et al. 2003. Mitochondrial dysfunction in the elderly: possible role in insulin resistance. *Science.* **300**:1140–1142.
50. Hancock, C.R., et al. 2008. High-fat diets cause insulin resistance despite an increase in muscle mitochondria. *Proc. Natl. Acad. Sci. U. S. A.* **105**:7815–7820.
51. Turner, N., et al. 2007. Excess lipid availability increases mitochondrial fatty acid oxidative capacity in muscle: evidence against a role for reduced fatty acid oxidation in lipid-induced insulin resistance in rodents. *Diabetes.* **56**:2085–2092.
52. Finck, B.N., et al. 2005. A potential link between muscle peroxisome proliferator-activated receptor-alpha signaling and obesity-related diabetes. *Cell Metab.* **1**:133–144.
53. Koves, T.R., et al. 2008. Mitochondrial overload and incomplete fatty acid oxidation contribute to skeletal muscle insulin resistance. *Cell Metab.* **7**:45–56.
54. Sinha, S., Perdomo, G., Brown, N.F., and O’Doherty, R.M. 2004. Fatty acid-induced insulin resistance in L6 myotubes is prevented by inhibition of activation and nuclear localization of nuclear factor {kappa}B. *J. Biol. Chem.* **279**:41294–41301.
55. Yuan, M., et al. 2001. Reversal of obesity- and diet-induced insulin resistance with salicylates or targeted disruption of Ikkbeta. *Science.* **293**:1673–1677.
56. Bloch-Damti, A., and Bashan, N. 2005. Proposed mechanisms for the induction of insulin resistance by oxidative stress. *Antioxid. Redox Signal.* **7**:1553–1567.
57. Henriksen, E.J. 2006. Exercise training and the antioxidant alpha-lipoic acid in the treatment of insulin resistance and type 2 diabetes. *Free Radic. Biol. Med.* **40**:3–12.
58. Moini, H., Tirosh, O., Park, Y.C., Cho, K.J., and Packer, L. 2002. R-alpha-lipoic acid action on cell redox status, the insulin receptor, and glucose uptake in 3T3-L1 adipocytes. *Arch. Biochem. Biophys.* **397**:384–391.
59. Lou, P.H., et al. 2007. Mitochondrial uncouplers with an extraordinary dynamic range. *Biochem. J.* **407**:129–140.
60. Kuznetsov, A.V., et al. 1996. Striking differences between the kinetics of regulation of respiration by ADP in slow-twitch and fast-twitch muscles in vivo. *Eur. J. Biochem.* **241**:909–915.
61. Tonkonogi, M., et al. 2003. Reduced oxidative power but unchanged antioxidative capacity in skeletal muscle from aged humans. *Pflugers Arch.* **446**:261–269.
62. Cheung, A., et al. 2002. A small-molecule inhibitor of skeletal muscle myosin II. *Nat. Cell Biol.* **4**:83–88.